This article is licensed under a Creative Commons Attribution-NonCommercial 3.0 Unported Licence.

RSC Advances



View Article Online **REVIEW**



Cite this: RSC Adv., 2018, 8, 20952

Stability of organometal halide perovskite solar cells and role of HTMs: recent developments and future directions

Ehsan Raza, Fakhra Aziz and Zubair Ahmad **

Perovskite solar cells (PSCs) have recently emerged as one of the most exciting fields of research of our time, and the World Economic Forum in 2016 recognized them as one of the top 10 technologies in 2016. With 22.7% power conversion efficiency, PSCs are poised to revolutionize the way power is produced, stored and consumed. However, the widespread use of PSCs requires addressing the stability issue. Therefore, it is now time to focus on the critical step i.e. stability under the operating conditions for the development of a sustainable and durable PV technology based on PSCs. In order to improve the stability of PSCs, hole transport materials (HTMs) have been considered as the paramount components. This is due to the fact that most of the organic HTMs possess a hygroscopic and acidic nature that leads to poor stability of the PSCs. This article reviews briefly but comprehensively the environmental stability issues of PSCs, fundamentals, strategies for improvement, the role of HTMs towards stability and various types of HTMs. Also the environmental parameters affecting the performance of perovskite solar cells including temperature, moisture and light soaking environment have been considered.

Received 23rd April 2018 Accepted 26th May 2018

DOI: 10.1039/c8ra03477j

rsc.li/rsc-advances

Recent advancement in PSCs

For the first time, in 2006, Miyasaka and co-workers¹⁻³ reported the potential use of perovskite as a light absorbing material (e.g. methylammonium lead bromine CH₃NH₃PbBr₃) in dye sensitized solar cells and stated the power conversation efficiency (PCE) as 2.2%.3 In 2009, they replaced bromine with iodine and demonstrated a slight increase in the efficiency i.e. 3.8%4 (all devices were unstable). Later, in 2011, Park and colleagues fabricated perovskite based highly efficient quantum-dot (QD) sensitized solar cells and reported a PCE of 6.5%.5 Despite a considerable leap in power conversion efficiency (PCE), 6 QDs tend to dissolve in the redox electrolyte. Hence, Park and Gratzel introduced the first solid-state mesoscopic solar cell based on perovskite nanocrystals, mesoporous TiO2 layers and spiro-MeOTAD as hole transporting material (HTM) and boosted the PCE to $9.7\%^7$ along with long term stability (\sim for 500 h). Afterwards, Snaith and co-workers introduced mesosuperstructured solar cells (MSSCs), in which they replaced non conducting Al₂O₃ with mesoporous conducting n-type TiO₂ and reported a PCE of 10.9%.8 An improvement in efficiency to 12% was reported after the combined efforts of M. K.

Nazeeruddin, Gratzel, Seok and co-workers.9 In their work, they introduced a layered sandwich type structure in which three dimensional nanocomposites of mesoporous (mp)-TiO₂, with methylammonium lead triiodide CH3NH3Pbl3 as light harvester and polymeric hole transport materials were used. Seok's group further improved efficiency to 12.3% with the same structure but mixed halide CH₃NH₃Pbl_{3-x}Br_x perovskites.¹⁰ For the first time, Huckaba et al.11 studied low cost TiS2 p-type contact material (30 times lower in price as compared to spiro-OMeTAD) as HTM, synthesized by a simple two step hot injection method and reported 13.5% PCE. In early 2013 during the European Materials Research Symposium, two groups reported efficiencies above 15%. 12 Gratzel's group reported 15% by using mesoporous TiO₂ and two-step sequential of lead iodide (PbI₂) with improved morphology. While Snaith's group reported 15.4% efficiency with better morphology.1 They used simple structure of $CH_3NH_3PbI_{3-x}Cl_x$ deposited by two-source thermal evaporation method. M. K. Nazeeruddin and group demonstrated 15.4% PCE using newly synthesized benzothiadiazole substituted derivatives, 4-(3,5-bis(trifluoromethyl)phenyl)-7-(5'hexyl-[2,2'-bithiophen]-5-yl)benzo[c][1,2,5]thiadiazole (CF-BTz-ThR) as HTM and aligned TiO2 nano bundles (TiO2 NBs) as ETL and fabricated high performance CH₃NH₃PbI₃ PSC. 13 M. K. Nazeeruddin et al.14 investigated low-temperature solution processable deoxyribose nucleic acid (DNA)-hexydecyl trimethyl ammonium chloride (CTMA) as HTM and (6,6)-phenyl C61butyric acid methyl ester (PCBM) as electron-acceptor layer in inverted p-i-n configuration based perovskite solar cells and reported 15.86% PCE. Late in 2013, Seok and co-workers used

^aDepartment of Electronics, Faculty of Physical and Numerical Sciences, University of Peshawar, Peshawar 25120, Pakistan

^bDepartment of Electronics, Jinnah College for Women, University of Peshawar, Peshawar 25120, Pakistan

^cCenter for Advanced Materials (CAM), Qatar University, 2713 Doha, Qatar. E-mail: zubairtarar@au.edu.aa

Review $CH_3NH_3Pb(I_{1-x}Br_x)_3$ as light harvester and poly(triarylamine) as HTM and gained 16.2%15 PCE. C. K. Teak and fellows tetra-tert-butyl ZnPc. substituted zinc phthalocyanines (ZnPcs) and tetra-5hexylthiophene- as hole transporting materials in mixed ion perovskite $[FAPbI_3]_{0.85}[MAPbBr_3]_{0.15}$ based solar cells and ZnPc and HT-ZnPc, respectively.16 Their work paved the way inexpensive energy production applications. Earlier in 2014,

studied easily accessible zinc phthalocyanines including tetra-5-hexyl-2,2'-bisthiopheneachieved PCEs of 13.3%, 15.5% and 17.5% for TB-ZnPc, HBTfor solution processed ZnPc derivatives as stable and cost effective hole transport materials for wide scale, efficient and again Seok and group members reported an efficiency of 17.9%. P. Sanghyun et al. designed star shaped D- π -A type HTMs including a rigid quinolizino acridine (FA-CN) and a flexible triphenylamine (TPA-CN) as central unit and donor part, alkyl-substituted terthiophene as a conjugated bridge and malononitrile as an electron acceptor. Dopant free FA-CN and TPA-CN based devices exhibited PCEs of 18.9% and 17.5%, respectively, under AM 1.5 illuminations. 18 M. K. Nazeeruddin and fellows demonstrated 19% PCE with stabilized performance for 1000 h under continuous light illumination by adding large organic cation guanidinium (Gua) into MAPbI3.19 For the first time, M. K. Nazeeruddin and fellows introduced a simple and highly reproducible approach to obtain highly efficient hybrid perovskite solar cells by combining 10% of formamidinium (FA) with methylammonium lead iodide (MAPbI₃) and reported 20.2% PCE.20 M. K. Nazeeruddin and group studied a combination of triple Cs/MA/FA cation by adding a small amount of inorganic cesium (Cs) and achieved highly efficient PSCs with stabilized PCEs of 21.1% and outputs at 18% under operational conditions after 250 hours.21 Their work opened the doors for other scientists and researchers to explore alkali metals like K, Li, Na and Rb as cations for perovskites. 21 Some researchers and scientists form Korea reported 22.1% PCE by introducing additional iodide ions into the organic cation solution.22 Recently in 2017, a team from Korean Research Institute of Chemical Technology (KRICT) developed a perovskite based solar battery cells and boosted the power conversion efficiency upto 22.7%18 (the highest PCE on record so far).

Ye et al.23 and fellows performed n-type doping of bis(1-[3-(methoxycarbonyl)propyl]-1-phenyl)-[6,6]C62 (Bis-PCBM) with decamethylcobaltocene (DMC). The device exhibited smooth surface morphology, good solvent resistance and improved device stability. The maximum PCE of 20.14% reported.²³ M. Qian and co-workers examined the device performance by anode modification in which they doped silver nano-particles (Ag NPs) with poly(3,4ethylenedioxythiophene):poly(4-styrenesulfonate) (PEDOT:PSS) and cathode interfacial modification by adding a solution processed bathophenanthroline (sBphen) in CH₃NH₃PbI_{3-x}Cl_x based PSC. Using this approach, they exhibited PCE as high as 15.75%.24 Z. Wang and fellows demonstrated solution processed PEDOT:PSS-GeO2 composite films as a hole transport layer in planar structure PSC. The device exhibited PCE of

15.15% and fill factor (FF) of 74%.25 Zheng et al.26 studied various solution processed interfacial layers of transition metal oxides (TMOs) including molybdenum oxide (MoO₃), vanadium oxide (V₂O₅), germanium dioxide (GeO₂) and chromium trioxide (CrO₃). Among these V₂O₅ film showed highest work function (5.2 eV) with best hydrophobic property at a contact angle of 72.2°. V₂O₅ based organic solar cells (OSCs) and perovskite solar cells (PSCs) exhibited PCEs of 8.36% and 14.13%, respectively. When used as a composite with PEDOT:PSS, the PEDOT:PSS:V2O5 based PSCs showed improved device performance with PCE of 18.03%. Wang et al.27 developed an efficient stable hole transport material tetrafluorotetracyanoquinodimethane (F4-TCNQ)-doped copper phthalocyanine-3,4',4",4"'-tetra-sulfonated acid tetra sodium salt (TS-CuPc) in planar structure PSCs by solution processing. Using TS-CuPc:F₄-TCNQ as the hole transporting material, they achieved PCEs of 16.14% for p-i-n structure and 20.16% for n-i-p structure, respectively. Li et al.28 developed copper salts (cuprous thiocyanate (CuSCN) or cuprous iodide (CuI)) doped spiro-OMeTAD based solution processed, stable hole transport materials. By p-doping they improved device performance and enhanced the PCE from 14.82% to 18.02%. Z. Wang and coworkers developed a thin perylene underlayer using solution processed method. The multifunctional perylene improved the overall device performance and significantly enhanced the PCE from 12.67% to 17.06.29 Such rapid improvement in less than 5 years suggests that organometal halide perovskites are indeed a new class of solar absorber. Fig. 1 provides the general view on the efficiency trends of perovskite solar cells from 2009 to 2017.

2. Stability of perovskite solar cell

Recently, over the past few years, hybrid organic-inorganic halide perovskites have been developed as potential candidates for photovoltaic applications. Device instability and degradation under ambient conditions restrict them for commercialization. Stability is currently one of the most investigated topics in PSCs. The devices that exhibited higher efficiencies comparable to silicon-based devices were degraded quickly. To improve the device stability, a basic understanding of the stability should be acquired. Factors that have an impact on the stability of perovskites have been explored. Normally, degradation in perovskites is caused by air (moisture & oxygen), UVlight, elevated temperature and chemical degradation as shown in Fig. 2. Here below, the stability has been categorized into two types which includes chemical stability and thermal stability.

2.1. Chemical stability

The chemical stability of perovskite solar cells refers to a series of chemical reactions under various conditions and atmospheres. The main factors that affect chemical stability in PSCs are oxygen, moisture and UV light. Many reports regarding aforementioned factors have addressed the degradation issues in PSCs. During the process of fabrication, testing and assembling, moisture and oxygen might have direct influence on the RSC Advances Review

Efficiency Trends & Associated Timeline

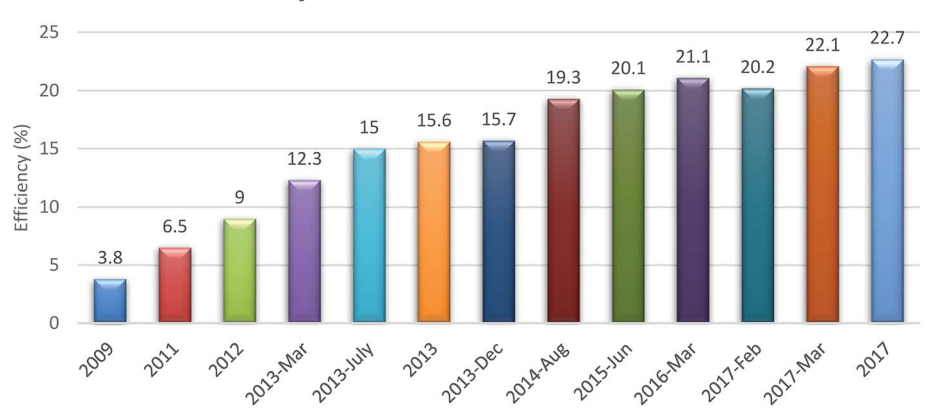


Fig. 1 General view on the efficiency trends of perovskite solar cells from 2009 to 2017

stability during the reaction process.^{30,31} Niu *et al.*³² studied the moisture effect on CH₃NH₃PbI₃ perovskite. They suggested that CH₃NH₃PbI₃ is highly sensitive to moisture and gets easily degraded.^{31,32} They presented degradation mechanism as mentioned below in eqn (1)–(4). They reported that in the presence of moisture CH₃NH₃PbI₃ decomposes into CH₃NH₃I and PbI₂ as shown in reaction (1). In reaction (2), CH₃NH₃I further decomposes into CH₃NH₂ and HI. HI can react in the following two ways. One way is using redox reaction method in the presence of oxygen (3). The second is photochemical method in which, HI breaks down into H₂ and I₂ under UV radiation as shown in reaction (4).

$$CH_3NH_3PbI_3 \leftrightarrow PbI_2 + CH_3NH_3I$$
 (1

$$CH_3NH_3I \leftrightarrow CH_3NH_2 + HI$$
 (2)

$$4HI + O_2 \leftrightarrow 2I_2 + 2H_2O \tag{3}$$

$$HI \leftrightarrow H_2 + I_2$$
 (4)

A similar impression was reported by Walsh *et al.*¹⁹ that MAPbI₃ is partially decomposed on exposure to moisture¹⁹. They proposed that a single molecule in H₂O known as Lewis base, reacts with MAPbI₃ and extracts one proton from ammonium leading to intermediates. Furthermore, these

Structural transformation

Thermal instability

Chemical instability

Fig. 2 Various factors which affect the stability in PSCs.

intermediates may decompose into HI, CH₃NH₂ and solid PbI₂. Gong et al.33 studied the degradation phenomena in perovskite solar cells. They reported DR3TBDTT as hydrophobic hole transporting material (HTM) with improved stability suggesting DR3TBDTT as moisture resistant potential candidate.33 Aristidou and co-workers studied the combined effect of light and oxygen on the stability of CH3NH3PbI3 perovskite. They observed that the reaction between superoxide (O₂⁻) and methylammonium moiety of the perovskite layer turned out to be the cause of degradation in CH₃NH₃PbI₃ perovskite.³⁴ Snaith et al.35 studied the stability in TiO2-sensitized mesosuperstructured solar cell (MSSC) under UV radiation for the first time. They identified the instability due to light induced desorption of oxygen which is adsorbed on the surface of mesoporous TiO2. The instability issue was resolved by implementing an insulating mesoporous Al₂O₃ scaffold as a substitute of n-type mesoporous TiO2. The Al2O3 based MSSC showed improved stability and stable photo currents under continuous full spectrum of sunlight over a period of 1,000 h.35 Hitoshi et al. 36 studied the stability of CH₃NH₃PbI₃ perovskite without encapsulation under one sun irradiation (AM 1.5). They observed that the decomposition appeared at the interface between TiO₂ and CH₃NH₃PbI₃. For this they proposed possible reaction at the interface between TiO2 and CH3NH3PbI3 as given in eqn (5)–(7):

$$2I^- \leftrightarrow I_2 + 2e^-$$
 [at the interface between TiO₂ and CH₃NH₃PbI₃] (5)

$$3CH_3NH_3^+ \leftrightarrow 3CH_3NH_2\uparrow + 3H^+ \tag{6}$$

$$I^{-} + I_{2} + 3H^{+} + 2e^{-} \leftrightarrow 3HI \uparrow$$
 (7)

As far as the stability under illumination is concerned, a study is conducted by adding Sb₂S₃ at the interface of TiO₂ and CH₃NH₃PbI₃. With addition of Sb₂S₃ as a surface blocking layer, the stability of CH₃NH₃PbI₃ was significantly improved.³⁶ Komarala *et al.*³⁷ demonstrated the UV degradation in TiO₂ based CH₃NH₃PbI₃ using down-shifting (DS) YVO₄:Eu³⁺ nanophosphor layer. The europium (Eu³⁺) doped yttrium vanadate (YVO₄) has a specific 4f electronic structure. This material

RSC Advances Review

converts absorbed UV light into visible light which is then absorbed by CH₃NH₃PbI₃. Using this approach, they achieved ~8.5% enhancement in the photocurrent and improved stability of PSC under UV light exposure.

2.2. Thermal stability

According to the International Standards IEC 61646, at 85 °C long term stability is required to compete with silicon-based technology. Several factors affect thermal stability in perovskites devices such as intrinsic temperature (due to perovskite material itself), electrodes degradation and charge transporting layers i.e. hole transport materials (HTM) and electron transport materials (ETM) degradation. Gratzel et al.38 examined the thermal behavior of the perovskite materials and analyzed thermal properties of their individual components. They observed the tetragonal to cubic phase transition in PbI₂ precursor based perovskite which might affect thermal stability in perovskite. Pisoni et al.39 studied the thermal conductive properties of MAPbI₃. In their experiments, large single crystals and polycrystalline samples showed very low thermal conductivity. Such low thermal conductivity could not allow light deposited heat to spread out quickly; this may cause mechanical stress and affect the performance of photovoltaic device. Snaith et al.40 investigated thermal and moisture stability in perovskites. They employed a new class of hole transporting material polymer-functionalized single-walled carbon nanotubes (SWNTs) embedded in an inert polymer matrix and achieved thermal stability. Conings et al.41 explored the intrinsic instability of perovskite material during heating at 85 °C. They reported the soft matter nature of perovskite layer by investigating morphological, electrical, chemical and optical characteristics of this new class of material. This experiment was performed in pure dry N2, pure dry O2 and at ambient atmosphere with 50% relative humidity for 24 h in the dark. 41 Their results revealed that degradation starts at 85 °C, and its rate is reliant on surrounding atmosphere.

Misra and co-workers demonstrated degradation in encapsulated MAPbl₃. They observed no degradation when MAPbl₃ was exposed to 1 suns (1 sun = 100 mW cm⁻²) at 25 $^{\circ}$ C for 60 minutes, while MAPbl₃ started degrading when the temperature rose from room temperature to 45-55 °C.42 N. G. Philippe et al. 43-45 investigated thermal stability by studying the ratios of I/Pb and N/Pb using hard X-ray photoelectron spectroscopy (HAXPES). The measurements were performed at room temperature, 100 and 200 °C for 20 minutes. As observed, MAPbl₃ started to decompose into Pbl₂ [eqn (8)] with increase in temperature from room temperature to 100 °C and then to 200 °C. The estimated I/Pb and N/Pb ratios gained form HAXPES results, revealed that MAPbl₃ to Pbl₂ ratio modified form 85:15 to 70:30 and to 0:100 respectively.43

$$MAPbI_3 \rightarrow PbI_2 + CH_3NH_2\uparrow + HI\uparrow$$
 (8)

Park et al.46 reported a good thermal stability in FAPbl₃ perovskite at an annealing temperature of 25 °C for 15 min. Similarly, Zhao et al.47 demonstrated excellent thermal stability in FAPbl₃ perovskite annealed at 160 °C for 80 min. Jin et al.48 proved that FAPbl3 is more thermally stable as compared to MAPbl₃ or any other perovskite.⁴⁹ Han et al.⁵⁰ introduced tetrathiafulvalene derivative (TTF-1) as a hole transporting material (HTM) into PSCs. They achieved 11.03% PCE with improved stability as compared to spiro-OMeTAD (PCE $\sim 11.04\%$). Meng et al.⁵¹ revealed stable perovskite device structure with no hole transporting layer (HTL) and achieved PCE of 10.5%. Similarly, Conings et al.41 and yang and co-workers reported thermal instability due to electron transporting layers i.e. ZnO and TiO2.41,52

3. Strategies for improving stability

Several strategies have been addressed in the literature that can be adopted to improve stability issues in PSCs.

3.1. Modification in perovskite structure

One of the proposed strategies to improve stability is to tune ABX₃ structure. Here A is a cation, B is a divalent metal ion and X is a halide. Seok et al. 10 have demonstrated an improved stability against moisture by controllable tuning of halide composition. Thiocyanate (SCN) group is a class of stable pseudohalogen having comparable properties of halogen. They can be used to tune the X halide composition to achieve best device stability. SCN⁻ has similar ionic radius as compared to I⁻. Y. Chen and co-workers introduced a planar cell structure using $MAPbI_{3-r}(SCN)_r$ and reported good device stability with remarkably high reproducibility.53 Without encapsulation, $MAPbI_{3-x}(SCN)_x$ retained 86.7% of its average efficiency at 70% RH for over 500 h, while MAPbI₃ lost 40% of its original efficiency.54

Few research groups proposed routes to improve stability by tuning methylammonium as a cation with inorganic. Fully inorganic cesium-based perovskite has gained interest due to its potential of tolerating elevated temperatures. CsPbX3 based perovskites have demonstrated outstanding thermal stability. Furthermore, cesium cation can also stabilize the FAPbI₃ crystal structure. Lee et al. 55 reported that cesium not only increases the efficiency via stabilization of black FAPbI3 perovskite phase but also improves film stability under light illumination and humidity environment. S. I. Seok's group demonstrated that under humid environment the stability of perovskite can be significantly enhanced by doping bromide with MAPbI3.31,56 They prepared (MPSC) devices using mixed halide perovskite $MAPb(I_{1-x}Br_x)_3$. To test the stability, the un-encapsulated devices were exposed to controlled humidity under ambient conditions. At 35% humidity, all devices exhibited no significant degradation in PCE. But when the humidity increased to 55%, MAPb $(I_{0.8}Br_{0.2})_3$ and MAPb $(I_{0.71}Br_{0.29})_3$ based devices showed good stability. On the other hand, MAPbI₃ and MAPb(I_{0.94}Br_{0.06})₃ based devices degraded rapidly. The devices based on MAPb($_{1-x}Br_x$)₃ ($x \ge 0.2$) exhibited enhanced stability under high humid environment due to compact and stable crystal structure.

RSC Advances

3.2. Addition of filters/thin layers

Another approach to increase stability of the perovskite devices against UV light and moisture is the addition of a very thin layer between the perovskite and hole transport layers or electron extracting layers. Several hydrophobic layers have been introduced as moisture barriers between the perovskite layers and spiro-OMeTAD. The purpose of these layers is to block any moisture diffusion through the hole transport layers to prevent device degradation. The layers should be thin enough to allow charge transfer and thick enough to block moisture ingress. An ultra-thin layer of Al2O3 was deposited between perovskite absorber and spiro-OMeTAD using atomic layer deposition (ALD). The device exhibited improved stability with 90% of the initial value at 50% RH for 24 hours without illumination. Guarnera et al.57 reported improved device performance and stability by introducing a spin-coated layer of alumina nanoparticles between the perovskite layer and spiro-OMeTAD. Ito et al.36 reported improved device stability under illumination by employing Sb₂S₃ as a buffer layer between perovskite absorber and TiO2. Li and co-workers stabilized the perovskite device by inserting a layer of CsBr between the perovskite and TiO2.58 Pathak et al. 59 developed Al-doped TiO2 and reported enhanced device stability and performance under full light exposure. Besides improved device stability, Al-doping has negative impact on charge extraction efficiency that results in a reduced photocurrent. To overcome this issue, neodymium (Nd) doping was introduced instead of Al doping. Nd-doped mesoporous TiO₂ based devices demonstrated steady state efficiency of 18.2% with improved stability as compared to their undoped counterparts. In order to improve the device photo-stability, Zheng and co-workers completely replaced TiO2 with CdS as an n-type layer. After continuous exposure of light for 12 h, CdS based devices retained more than 90% of their initial efficiency, while TiO2 based devices experienced a decrease in their efficiency from 15.4 to 3.1%.60

To solve the stability issues for perovskite solar cells, a novel interface engineering approach was introduced by J. Chen and group members. In which they developed a versatile ultrathin 2D perovskite (5-AVA)2PbI4 (5-AVA = 5-ammoniumvaleric acid) passivation layer at back contact between perovskite and CuSCN interface. By using back contact interface engineering, they achieved improved device performance along with photo and moisture stability.61

Role of HTM in stability 4.

The HTMs are the major components of the PSCs which have much effect on the stability of PSCs. Stability depends on hydrophobic property and morphology of the HTM as well as the interface between HTM and perovskite layer. Organic HTMs are used in the most efficient perovskite solar cells. Hole transportation and retardation of charge recombination are their main function. So far, HTMs in perovskite solar cells mainly involve nitrogen-based donors such as 2,2',7,7'-tetrakis-(*N*,*N*-di-*p*-methoxyphenylamine)-9,9'-spiro-bifluorene (spiro-OMeTAD), poly-(triarylamine) (PTAA), and so on. Due to the

triangular pyramid configuration of sp3 hybridization of nitrogen atom, large intermolecular distances are present in the structure. As a result, they suffer from low hole mobility, low conductivity, or both, in their pristing form. Therefore, "redox active" p-type dopants, such as Li-bis(trifluoromethanesulfonyl) imide (Li-TFSI), have been commonly adopted to increase conductivity and thereby improve cell performance. However, such dopants have aggravated cell performance degradation because of their tendency to become liquid or to absorb moisture from air and get dissolved in the moisture. J. Liu et al.50 used tetrathiafulvalene derivative (TTF-1) as a hole transport material (HTM) in a perovskite solar cell. The HTM did not use any dopant and resulted in the stability better than the one that uses spiro-OMeTAD, a p-type dopant.

For instance, M. K. Nazeeruddin and co-workers reported molecularly engineered star-shaped D- π -A dopant free hole transport materials comprising rigid quinolizino acridine (FA-CN) and a flexible triphenylamine (TPA-CN). By this approach, they observed improved device efficiency and significantly enhanced stability as compared to doped spiro-OMeTAD under light soaking (100 mW cm⁻²) conditions.⁶² In an atom or atomic lattice, electron hole or hole is the absence of electron at a position where an electron could exist. For example, helium has two electrons in its atom, if an electron leaves helium, an electron hole is created. This also makes the helium atom positively charged. In metal, electrons and electron holes move in a similar way. In an electric field, the movement of holes slows down and results in slow performance of the electronic device. Further, F. Zhang and fellows synthesized and characterized two novel thiophene based HTMs, Z25 and Z26 and demonstrated a simple strategy by adding double bonds to the structure of hole transporting layers. This double bonding benefits hole mobility in Z26 based device which improves PCE to 20.1% and the device was more stable than Z25 and spiro-OMeTAD based devices.63

5. Hole transport materials (HTMs)

Solid state hole transport materials can be categorized into three main classes: organic, inorganic and hybrid. Table 1 provides a close look on the HTMs with their efficiencies and stabilities. Each type has different pros and cons, which will be discussed in the following sections.

5.1. Organic hole transport materials

Organic hole transport materials can be further categorized into small molecule HTMs and polymeric HTMs.

5.1.1. Small molecule HTMs. Low molecular weight organic materials are economical, simple to synthesize, easy to modify and possess solution processable nature.81 This section review summarizes the research on small molecule HTMs used in standardized PSCs device structures. Spiro-OMeTAD (Fig. 3) is one of the most widely used organic small molecular HTMs and has produced highly efficient devices.81 The problem with spiro-OMeTAD is its cost and poor hole mobility. To overcome these factors many HTMs have been introduced with almost

Table 1 Types of HTMs along their efficiencies and stability

Name	Efficiency	Stability	References
Spiro-OMeTAD	20.6%	_	_
P3HT	20%	800 h	64
Z25	16.9	Higher than spiro-OMeTAD (300 h)	63
Z26	20.1	Higher than spiro-OMeTAD (800 h)	63
DBTP	18.09	Higher than spiro-OMeTAD (81% retention after 792 h or 33 days)	65
TTA	16.7	Tested for 300 hours	66
SYN1	11.4	Outclass performance than spiro-OMeTAD based devices (value not mentioned)	67
PARA1	13.1	Outclass performance than spiro-OMeTAD based devices (value not mentioned)	67
TPA-ZnPC	13.65	Higher than spiro-OMeTAD (value not mentioned)	68
Q221	10.37	200 h	69
Q222	8.87	200 h	69
ZnPcNO ₂ -OPh	14.35	Higher than spiro-OMeTAD (tested for 33 days, PCE decreased to 4%)	70
CuPcNO ₂ -OPh	12.72	Higher than spiro-OMeTAD (tested for 33 days, PCE decreased to 18%)	70
Ag:NiOx	16.86	Higher than organic HTM (tested for 30 days, PCE mentioned over 80%)	71
BPNS	16.4	Lower than spiro-OMeTAD	72
PEDOT:PSS	20	Higher stability than pristine PEDOT:PSS based HTM	73
MoO_2	15.8	Shows high stability in moisture	74
Triazatruxene	15	Hydrophobic in nature (value not mentioned)	75
PVK	12.1	Tested until 1000 h (more stable than PEDOT:PSS)	76
Me-QTPA	9.07	Higher than spiro-OMeTAD (tested for 600 h. Shows hydrophobicity)	77
Me-BPZTPA	8.16	Tested for 600 h	77
FePc-Cou	9.40	Tested for 10 h	78
NiPc-Cou	10.23	Tested for 10 h	78
DEPT-SC	11.52	Tested until 250 h	79
TTPA-BDT	18.1	Show good thermal stability (value not mentioned)	80
TTPA-DTP	15.6	Show good thermal stability (value not mentioned)	80
TEOS	_	(Stable for 1200 hours)	77

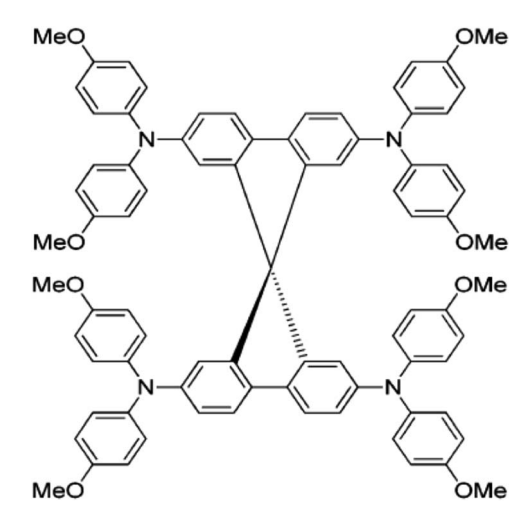


Fig. 3 Molecular structure of spiro-OMeTAD. This figure has been adapted from ref. 82 with permission from American Chemical Society.

same features as offered by spiro-OMeTAD, which are discussed below.

Pyrene core and truxene core based HTMs. First, alternate HTMs appeared in 2013 by Seok et al.⁸² The pyrene core (as given in Fig. 4) was introduced in arylamine derivative molecules and it replaced the spiro-bifluorene core in spiro-OMeTAD. The three categories of pyrene achieved PCE of 3.3%, 12.3% and 12.4% for PY-1, PY-2 and PY-3 respectively, while under same conditions the spiro-OMeTAD exhibited PCE

of 12.7%. The lower PCE (3.3%) for PY-1 was due to insufficient hole injection. The addition of pyrene core in arylamine derivatives introduced electron-blocking capability surpassing that of spiro-OMeTAD, while keeping synthesis cost lower.82 Chen et al.83 developed a C3h truxene-core (Trux-I) using OMeTAD. Its distinct structure resulted in an excellent hole mobility, greater than the spiro-OMeTAD. Grisorio et al.84 further modified the Trux-I and synthesized a new molecule Trux-II. In the case of p-in device structure both Trux-I and Trux-II exhibited better performance with PCE for Trux-I = 10.2%, Trux-II = 13.4% as compared to the reference samples using spiro-OMeTAD (with 9.5% PCE). Rakstys et al.85 have synthesized two-dimensional triazatruxene-based derivatives series (triazatrux I-IV) using a simple synthesis procedures to produce low cost devices. Among this series triazatrux-II structure exhibited PCE of 17.7%, while spiro-OMeTAD based reference device showed PCE of 17.1%.

Fig. 4 Molecular structure of pyrene-based HTMs. This figure has been adapted from ref. 82 with permission from American Chemical Society.

RSC Advances Review

Phenothiazine based HTMs. Phenothiazine is an important candidate in designing high-mobility organic semiconductors. See Structure of phenothiazine based HTMs is shown in Fig. 5. Recently, Grisorio and group developed and made two phenothiazine based (PH-I and PH-II) molecules. When used as HTMs, PH-I realized PCE of 2.1% whereas PH-II showed PCE of 17.6% which is very near to 17.7% for spiro-OMeTAD.

Thiophene, bithiophene and tetrathiophene HTMs. Liu et al. 88 have developed thiophene based HTMs (Thio-I and Thio-II) using dibromo thiophene and arylamine. PCE of 15.13% was achieved for Thio-II HTM which was 40% higher than that of Thio-I. Under same conditions spiro-OMeTAD as HTM surprisingly produced a PCE of 8.83%. Whereas, Rakstys et al. 89 prepared a bi-thiophene based derivative known as BTHIO. BTHIO based devices unveiled 19.4% PCE which was a slightly higher PCE (with improved stability) than that of reference device using spiro-OMeTAD. Also, Zimmermann et al. 90 established electron rich tetra-thiophene based HTMs (TETRATH I-IV). TETRATH-I reported 18.1% PCE along with higher thermal stability as compared to spiro-derivative. The results indicated that high performance, thermal stability and low-cost PSCs can be designed using tetrathiophene.

Triazine based HTMs. 12.5% and 10.9% PCEs were reported for TRIAZ-I and TRIAZ-II (as shown in Fig. 6) respectively reported by Ko and group. Lim *et al.* introduced two triazine-core star-shaped HTMs known as TRIAZ-III and TRIAZ-IV. They observed enhanced PCEs of 13.2 and 12.6% for TRIAZ-III and TRIAZ-IV, respectively, which are close to 13.8% achieved using spiro-OMeTAD.

Benzotrithiophene and squaraine HTMs. Ontoria et al. ⁹³ have acquired three benzotrithiophene based HTMs (BZTR-I, BZTR-II and BZTR-III) using cross-coupling reactions between various benzotrithiophene and triphenylamine derivatives with 18.2% PCE. In a simmilar manner, Benito et al. ⁹⁴ have designed tri-arm (BZTR-IV) and tetra-arm isomers (BZTR-V). The corresponding PSC devices exhibited outclass performance and achieved PCEs of 19 and 18.2% for BZTR-IV and BZTR-V, respectively with good stability under temperatures upto 430 °C. Recently, Paek et al. ⁹⁵ developed squaraine-based HTMs (SQ-H, SQ-OC₆H₁₃). From these HTMs, PCEs of 14.74% for SQ-H and 14.73% for SQ-OC₆H₁₃ were obtained while under same conditions the spiro-OMeTAD produced 15.33% PCE.

Fluorene and spiro-fluorene HTMs. Rakstys et al.96 developed bifluorenylidene based HTM (FL-I) with a lower band gap and a HOMO level similar to spiro-OMeTAD. FL-I, 50-times less expensive than spiro-OMeTAD, showed a PCE of 17.8%, which is comparable to 18.4% produced by spiro-OMeTAD. To enhance the electrical conductivity of the device, different dopants were used in HTMs which decreased the stability while increasing cost of the device. Keeping this in view, Wang et al. 97 developed a dopant free HTM (FL-II) which comprised of polytriarylamine unit (N-benzene) and spiro-OMeTAD. FL-II exhibited a PCE of 12.39% without dopants and 16.73% with dopants. While on other hand 14.84% and 5.91% values were reported using spiro-OMeTAD. Considering the device stability, Reddy and group introduced two fluorene based HTMs (FL-III and FL-IV) by Suzuki coupling reaction. Both, FL-III and FL-IV showed high hole mobility, good solubility and long-term device stability. These materials have been employed as substitute of spiro-OMeTAD in PSCs and substitute of PEDOT:PSS in organic bulk-heterojunction (BHJ). In PSC, the reported PCE was 17.25% for FL-III. While for BHJ it was 7.93%. The reference PCEs were 16.67% and 7.74% for spiro-OMeTAD and PEDOT:PSS, respectively.98 Tiazkis et al.99 have examined the characteristics of fluorene based HTMs. They observed that by replacing an aliphatic group to the meta- and para-positions of triphenylamine fragments, the charge transport, hole extraction and molecular planarity properties could be modified. In meta- substitution case, they observed inferior performance because of the non-favorable geometry, but in case of para-substitution, recorded PCE values were in the range of 9-16.8%, almost approaching the PCE of spiro-OMeTAD as a reference (17.8%).

Spiro-FL-I was designed by Bi and co-workers with excellent recorded PCE of 19.8%, comparable to that of spiro-OMeTAD (20.8%) reference sample. Also, FL-I based devices exhibited less hysteresis, outstanding reproducibility and better stability under specific (dry and dark) conditions. ¹⁰⁰ Keeping in view similar design structure, 3D-spiro-fluorene-based HTMs (spiro-FL-III and spiro-FL-III) were designed by Xu *et al.* ¹⁰¹ Spiro-FL-III showed higher hole-mobility, deeper HOMO level, better solubility and improved film properties as compared to spiro-OMeTAD. The spiro-FL-III also yielded impressive PCE of 20.8% much higher than the 18.8% PCE of spiro-OMeTAD with

Fig. 5 Structure of phenothiazine based HTMs. This figure has been adapted from ref. 86 with permission from Springer Nature.

Fig. 6 Structure of triazine based HTMs. This figure has been adapted from ref. 91 with permission from Royal Society of Chemistry.

magnificent stability after six months long-term aging. However, the spiro-FL-II achieved PCE of 13.6% with same order of hole mobility as does the spiro-OMeTAD. The overall materials cost was around 1/5 as compared to spiro-OMeTAD. The reported PCE values for these HTMs were upto 20%. Saliba *et al.* 103 have proposed a new class of HTMs FDT. When used as HTM in mesoscopic type configuration, the device exhibited highest PCE of 20.2% for small molecule HTMs. FDT are less expansive (\sim \$60 g⁻¹) and soluble in toluene that is less hazardous than chlorobenzene, which is used to dissolve spiro-OMeTAD.

TRIAZ-III

Carbazole based HTMs. The attractive photophysical properties like intense luminance, reversible oxidation process, low synthetic cost, flexible carbazole reactive sites and the outstanding charge transport properties make this class of compounds prominent and novel for cost effective HTMs for PSCs.^{67,104–114} Wang *et al.*¹¹⁵ reported a carbazole based CA-I compound made by a two-step reaction process using less expensive commercially available materials. CA-I, exhibited

good hole mobility and better conductivity than spiro-OMeTAD and showed a PCE of 12.3%. ¹¹⁶ Leijtens *et al.* ¹⁰⁶ have designed two, simple lithium salt-free, carbazole based HTMs, varied by the alkyl group (CA-II and CA-III). When applied in the PSCs in oxidized form, the devices produced results comparable to spiro-OMeTAD based devices. Other examples include two arms and three arm structures, connected *via* TPA, phenylene or diphenylene core units (CA-IV, CA-V and CA-VI). Using these systems, the highest PCE of 14.79% was achieved. Wang *et al.* ¹⁰⁸ developed carbazole based derivatives (CA-VII and CA-VIII) with biphenyl core.

TRIAZ-IV

Xu *et al.*¹¹⁴ have demonstrated two carbazole-core based HTMs (CA-IX and CA-X). Under similar conditions, in solid state DSSCs, CA-X based device achieved PCE of 6%, higher than that of CA-IX (4.5%) and spiro-OMeTAD (5%) as a reference. Due to superior performance of CA-X as compared to CA-IX and spiro-OMeTAD in solid state DSSC, CA-X was further investigated in PSC as HTM and achieved PCE of 9.8% as compared to 10.2%

RSC Advances Review

PCE obtained by spiro-OMeTAD based device as a ref. 117. Kang et al. 109 have designed a group of dendritic carbazole based star shaped HTMs (CA-XI, CA-XII and CA-XIII) and studied their performance in PSCs. Because of crystallization during the fabrication process, the trimeric structures showed good conductivity than the dimeric ones. When used as HTM, CA-XIII exhibited a PCE of 13% which is comparable to PCE of 13.76% achieved by spiro-OMeTAD based PSC. Zhang et al. 67 developed two new carbazole based materials (CA-XIV and CA-XV) utilizing commercially available di-substituted and tri-substituted phenyl derivatives. The CA-XV based PSC achieved slightly higher PCE of 13.1% as compared to 11.4% and 12.0% for CA-XIV and spiro-OMeTAD, respectively. Daskeviciene et al. 110 proposed a simple one-step synthesis for a low cost HTM (CA-XVI). When used as HTM, the PSC exhibited PCE of 17.8%, comparable to a reference device of spiro-OMeTAD. Chen et al. 111 proposed a tetra-substituted carbazole-based HTM (CA-XVII) using a three-step synthesis process and low-cost materials, which produced a PCE of 17.81%. Zhu and fellows have designed a carbazole-based molecular material using a tetraphenylene core (CA-XVIII). The device showed good thermal stability and energy levels with a PCE of 12.4%. The achieved PCE is close enough to the one obtained from doped spiro-OMeTAD device.112 Zhu et al.113 recently synthesized a chain of carbazole derivatives having variation in the 2,7 and 3,6 positions (CA-XIX, CA-XX and CA-XXII). Among these materials, the 2,7 substituted derivatives (CA-XX and CA-XIX) resulted in good stability because of highly twisted structure and PCEs of 16.74% and 14.92%, respectively. While 3,6 substituted derivative CA-XXII reported a PCE of 13.3%. Recently, Wu et al.118 have proposed a carbazole based HTM including electron deficient benzothiadiazole (BT) core (CA-XXIII). The addition of a BT unit in biphenyl structures in CA-XXIII increased the intermolecular interactions, improved hole mobility, charge transport and thermal stability of the compound. When used as HTM, a PCE of 16.87% was reported for CA-XXIII, higher than 15.53% achieved by spiro-OMeTAD PSC.

Hole transporting materials based on benzodithiophene and dithienopyrrole cores. M. K. Nazeeruddin et al.80 have observed and designed two new classes of HTMs based on benzodithiophene (BDT) and dithienopyrrole (DTP) cores. They substituted BDT and DTP central cores with four N,N-bis(4-methoxyphenyl) aniline units through the 2- and 3-positions of thiophene rings giving rise to the tetrakistriphenylamine (TTPA) derivatives. The substitution of the inner core benzene ring of BDT by a pyrrole ring in DTP allows addition of an extra heteroatom to the system, which provides a stronger electron donating characteristics. They reported that HTM based on BDT core demonstrated outclass performance with 18.1% as compared to DTP based HTM (15.6%) and spiro-OMeTAD based device (17.7%). This superior performance of TTPA-BDT based HTM was achieved due to better alignment of HOMO (-5.36 eV) with the perovskite's valence band (-5.65 eV), lower reorganization energy (0.1.1 eV) and higher fill factor.

Other small molecular materials HTMs. Zong et al.⁶⁹ have introduced two binaphthol based derivatives (NPH-I and NPH-II) which vary in the aromatic or aliphatic linkage to

binaphthol unit. The HOMO levels of both materials were well aligned with that of perovskite and PCE values reported were similar to that of spiro-OMeTAD. Li *et al.* ¹¹⁹ have designed two different HTMs by varying π -linker unit (biphenyl vs. carbazole: OMe-I and OMe-II) and obtained PCEs of 16.14% and 18.34% for OMe-I and OMe-II, respectively. Petrus *et al.* ¹²⁰ have studied the problem of reducing HTM synthetic costs. They introduced a material with 3,4-ethylenedioxy thiophene (EDOT) as a central core (EDOT-AZO). EDOT-AZO was synthesized under ambient conditions using simple one-step Schiff base condensation chemistry of amine and aldehyde of EDOT with cost effective precursors. EDOT-AZO is the least expensive HTM reported so far in the context of PSCs (cost of EDOT-AZO is around \$10 g^{-1}). As an HTM, EDOT-AZO reported a PCE of 11% comparable to 11.9% as obtained by spiro-OMeTAD based device.

5.1.2. Polymer hole transport materials. Poly(triaryl amine) (PTAA) was the first ever and the most efficient polymer based HTM, which was tested in PSCs. Seok et al. 104 used PTAA in mesoscopic structure and formed a zig-zag-like pattern; the reported PCE was 12%. Using mixed perovskites (MAPbBr₃ and FAPbI₃) and immense optimization process, the PCE was enhanced to 20%.121,122 Furthermore, PTAA is a high cost material (~\$2000 g⁻¹).123 P3HT and PEDOT:PSS are prominent conducting polymers and have been employed as HTMs.124 PEDOT:PSS has been mostly employed in inverted planar PSCs and possesses features like compatible valence band with perovskite, low temperature processability and excellent film properties. The highest efficiency of 18.1% was achieved using PEDOT:PSS with hydrogen iodide (HI) as additive and perovskite.125 The main constraint of PEDOT:PSS is its hygroscopic nature.

The improvement of the device stability through the introduction of the stable and efficient conducting polymer-based HTMs have been documented by Lim $et~al.^{126-128}$ They reported the use of high-work function self-organized hole extraction layers (SOHELs) to attain the improved PCE. ¹²⁸ A SOHEL accomplishes good energy level alignment with ionization potential level of $CH_3NH_3PbI_3$ in such a way that it increases built-in e-potential, J_{sc} , FF and V_{oc} . ^{126,128} They also compared the results of the PEDOT:PSS based PSCs with those incorporating SOHEL ¹²⁷ and found that the offset energy at the hole extraction layer and the photoactive layer can be reduced by collective energy level alteration of the SOHEL. They also made-up a flexible PSC on PET/ITO substrate using SOHEL and reported the PCE as high as 8.0%. ¹²⁸

Dubey *et al.* ¹²⁹ reported a diketopyrrolopyrrole based polymer known as PDPP3T and achieved a PCE of 12.32% comparable to 12.34% reported for spiro-OMeTAD based PSC. An additional interesting attribute, the PDPP3T based PSC produced slower device degradation having a decrease in PCE to 60.6% of its initial value in 172 h. On the other hand, spiro-OMeTAD based device decreased the PCE to 83% of its initial level in the same time. Stringer *et al.* ¹³⁰ have reported a carbazole based co-polymer, PCDTBT, a familiar donor material in organic BHJ devices. The PCDTBT device after being doped with LiTFSI and TBP achieved a PCE of 15.9% almost equal to that of spiro-OMeTAD device. Yu *et al.* ¹³¹ investigated a co-polymer

Review RSC Advances

based on PCPDTBT. The highest ever reported PCE of 15.1% achieved for PCPDTBT based polymers, when PCPDTBT 2,3,5,6-tetrafluoro-7,7,8,8was doped with tetracyanoquinodimethane (F4TCNQ). Zhou et al.132 have designed a hyper-branched carbazole based polymer (HB-CZ) using one-step Suzuki coupling method. When employed as HTM, the device showed a PCE of 14.07%, higher than the PCE of 9.05% and 6.60% reported for P3HT and PCz based devices, respectively. Liu et al. 133 have proposed a highly π -extended copolymer PDVT-10 as HTM with an excellent hole mobility of 8.2 cm² V⁻¹ s⁻¹ and achieved a PCE of 13.4% without doping that is considered the highest reported PCEs for dopant-free polymer HTMs.

Liu and fellows have proposed a carbazole based non-conjugated polymer (PVCz-OMeDAD), having a non-conjugated polyvinyl sequence and a hole transporting OMeDAD unit. The OMeDAD moiety increased hole transporting potential of the material. The PCE of 16.09% was observed, which is, much better than that of 9.62% obtained by spiro-OMeTAD based device used as a reference. Gaml $et\ al.^{134}$ have implemented benzodithiophene based polymer PBDTT-FTTE, as hole transporting material in PSCs. After doping, 3% of diiodooctane with PBDTT-FTTE, the device exhibited same performance as traditional spiro-OMeTAD based devices in an inert atmosphere with increased FF and $V_{\rm oc}$. Diiodooctane doped PBDTT-FTTE device achieved a PCE of 11.6%, whereas on the other hand the un-doped PBDTT-FTTE based cells exhibited a PCE of 10.3%.

5.1.3. Dopant free hole transport materials. Hole transportation materials (HTMs) play a key role in the performance of highly efficient PSCs. As mentioned earlier, spiro-OMeTAD has been the most widely used HTM. But, spiro-OMeTAD suffers an insufficient hole transportation and low conductivity in its pristine form. Therefore, additives/dopants like lithium bis(trifluoromethanesulfonyl)imide (Li-TFSI), ^{24,25,26} 4-tert-butylpyridine (TBP), ²⁶ and tris(2-(1*H*-pyrazol-1-yl)-4-tert-butylpyridine)cobalt(III) tri[hexafluorophosphate] (FK209)²⁶ are used to generate free carriers and to enhance conductivity. However, these dopants affect the device performance and stability.

For this purpose, the development of cost effective dopant free HTMs with improved moisture resistance and carrier transport properties is required for stable and efficient PSCs. Huang et al.83 demonstrated PCE of 18.6% using a dopant free HTM Trux-OMeTAD, comprising C_{3h}, Truxene-core with arylamine terminals and hexyl side chains. M. K. Nazeeruddin et al.62 introduced rigid quinolizino acri-dine (FA-CN) and a flexible triphenylamine (TPA-CN) as dopant free HTMs and exhibited PCEs of 18.9% and 17.5% for FA-CN and TPA-CN, respectively, under full sun illumination. M. K. Nazeeruddin and fellows successfully developed three symmetrical dopantfree HTMs (KR321, KR353 and KR355) using D- π -A type architecture. Among these three HTMs, the optimized structure of KR321 based device showed improved performance with a PCE of ~19% along with improved stability. 135 Heo et al. 136 investigated DFBT (DTS-FBTTh₂)₂ dopant free HTM using D'-A-D-A-D-A-D' (D, D': electron donors, A: electron acceptor)

conjugated structure and achieved 17.3% PCE. Lee and group members demonstrated 18.3% PCE using green solvent processable polymer HTM composed of benzothiadiazole (BT) and benzo[1,2-*b*:4,5:*b*']dithiophene (BDT) (asy-PBTBDT).¹³⁷

5.2. Inorganic hole transport materials

From the past several years, inorganic materials have been studied and implemented as hole transporting materials due to their unique properties such as appropriate energy levels, good hole mobility, high chemical stability and low fabrication cost. However, problem associated with this type of HTMs is the device stability introduced by a solvent, which can partially dissolve the perovskite. Nickel oxide (NiO) is the most promising wide band gap p-type material that was successfully used as HTMs in DSSC and OPV devices. It has been implemented in various device structures, like mesoporous carbon electrodebased PSCs, inverted mesoscopic PSCs and inverted planar based PSCs. Sarkar et al.138 achieved a PCE of 7.26% by depositing NiO layer on an inverted planar type configuration using electrodeposition. Chen et al. 139 enhanced the performance of NiO layer and achieved PCE of 11.6% under one-sunillumination by varying the thickness and using oxygen doping. Recently, low temperature solution processed NiOx was implemented as HTM in n-i-p and p-i-n PSCs structures. The considerable accomplishment of this work was to present direct deposition of pre-synthesized NiOx on the top of perovskite layer (in n-i-p assemblies) without rotting the perovskite film. The considerable PCE of 15.9% was obtained with negligible hysteresis.140 Duc et al.141 used NiO as HTM in perovskite based inverted planar configuration and reported a PCE over 16%.

Copper (Cu) has also been successfully investigated to design cost effective and solution processable Cu based inorganic HTMs. Kamat et al. 142 studied copper iodide (CuI) based device and reported overall PCE of 6%. The low efficiency was due to low $V_{\rm oc}$. Other interesting examples of this class of materials include cupric cuprous oxide (Cu2O) and copper thiocyanate (CuSCN). Cu₂O is a narrow band gap, low cost, environmental friendly material with good hole mobility. For such type of material, the reported PCE was 8.93% with good stability over 30 days in the open air. 143,144 In 2014, Gratzel et al. 145 performed considerable work on CuSCN as HTM and achieved 12.4% PCE. CuSCN HTM demonstrated performance owing to effective charge extraction and charge transportation from perovskite layer to top electrode. Moreover, a considerable PCE over 16% was reported by Nazeeruddin et al. 146 for PSCs using mixed perovskite (FAPbI3 and MAPbBr3) in addition to CuSCN as ptype hole transport material.

5.3. Hybrid hole transport materials

Y. Kwon used poly[2,5-bis(2-decyldodecyl)pyrrolo[3,4-c]pyrrole-1,4(2H,5H)-dione-(E)-1,2-di(2,20-bithiophen-5-yl)ethene] (PDPPDBTE) as a p-type HTM on a hybrid organic–inorganic perovskite solar cell. ¹⁴⁷ The hydrophobicity of the polymer prevented moisture permeation on the porous perovskite heterojunction. Z. Fei *et al.* ⁶³ used thiophene based HTMs (Z25, Z26) to achieve 20.1% efficiency which is similar to spiro-OMeTAD. The

RSC Advances Review

HTM Z26 showed more stability than spiro-OMeTAD and Z25. The presence of a double bond in the structure of Z26 made the HTM more stable. Thiophenes are semi-conductors in nature. Higher hole mobility of thiophene make them an attractive HTM material. Their interaction with iodine promote photogenerated hole transport. X. Liang et al. 148 argues that HTMs with high thermal stability and high hole mobility are rare. Phenothiazine based HTM, SFX-PT1 and SFX-PT2, were developed and found to be more stable than spiro-PT and spiro-OMeTAD. Moreover, SFX-PT1, SFX-PT2 and perovskite have comparable energy levels which make them compatible. However, SFX-PT1 and SFX-PT2 showed low solubility, which might be a problem for large scale application.

According to W. Yei et al.71 HTM made of silver doped NiOx(Ag:NiOx) showed better performance for an inverted planar heterojunction perovskite solar cell. In Ag:NiOx, Ag occupies the substitutional Ni sites and behaves as an acceptor in NiO lattice. Doping with silver increases hole mobility, conductivity and stability of NiOx film. The stability of this novel HTM compared to organic HTMs is drastically higher. Xie et al. 149 reported a high efficiency HTM $\text{Li}_{0.05}\text{Mg}_{0.15}\text{Ni}_{0.8}\text{O}$ as an alternative to original NiOx, which is attributed to enhanced hole conductivity and charge extraction. According to K. Im, Ti doped MoO2 has high thermal stability due to strong Mo-O bond.74 Moreover, the compound is highly stable in humidity as well. Another advantage of this HTM is its scalability. Although the compound is stable in humidity, MoO2 has the tendency to oxidize itself to MoO₃ in the air. However, doping with titanium solves this problem to some extent.

H. Li et al. 150 reports similar stability of 3,4-ethylenedioxythiophene and 9'-spirobifluorene (spiro-OMeTAD) which is a widely used HTM. Habisreutinger et al.40 proposed polymer-functionalized single walled carbon nano-tube (SWNT) embedded in an insulating polymer matrix as HTM. Strong retardation of thermal degradation was observed in the cell as compared to organic HTMs. Moreover, the proposed HTM was found to be water resistant. Perovskite and organic HTMs degrade fast under heat. If poly(methyl methacrylate) (PMMA) is used for coating perovskite, its thermal stability increases. But, the coating acts as an insulator as it lacks π -conjugation. However, combining this insulator with highly conductive single walled carbon nano-tube, the properties of conventional HTMs can be achieved along with durability. Carbon nanotubes (CNTs) are generally insoluble, however when wrapped with a monolayer of P3HT, they form supramolecular nano-hybrids (P3HT/SWNT) that are dispersible in common solvents and can be deposited by spin-coating.

Limitations of HTMs 6.

Organic HTMs have several drawbacks including unspecified molecular-weight, low purity and batch-to-batch variation. 105,151,152 The amorphous nature of small molecule-based hole transport materials imparts poor hole mobility. Among organic HTMs, polymers are well known for their good hole mobility, strong chemical interaction with perovskite and highest efficiency. These material have high molecular weight

which doesn't allow easy penetration hooked on the openings of TiO2 scaffold.152 Similarly, PEDOT:PSS with successful outcomes has a well knows drawback of hygroscopic nature, which restricts the chemical-stability of PEDOT:PSS based devices in an ambient environment. 152 In case of hydrophilic materials, all deposition processes need to be carried out in gas filled glove box and the measurements are performed with relative humidity (%RH) < 1 and under controlled atmospheric conditions.12 To solve this problem, several types of dopants are used. Unfortunately, these dopants decrease device stability and ultimately degrade the PSCs. 152 For the process of hole extraction, adequate hole transportation and conductivity are required. In regular n-i-p structures, a thick HTM layer is normally deposited to acquire a pinhole free surface on the perovskite. But, a thick HTM layer produces high series resistance that leads to lower FF and PV performance. To overcome this issue, p-type doping is commonly used to enhance hole mobility and conductivity of HTMs. However, an introduction of additives can affect the device stability, especially for hydrophilic components that can degrade the perovskite crystals. 153 In case of inorganic hole transport materials, the most common problem is their solvents which can partially dissolve the perovskite and consequently affect device performance and stability.152 Whereas the transition metal oxides as HTMs hold a very impoverished film morphology which results in extremely low quality films.152

7. Research agenda for future studies

The hole transport materials have significant effect on open circuit voltage (V_{oc}) of the cells as they decrease recombination resistance and increase series resistance. Apart from the properties and improved efficiencies several challenges need to be addressed before the successful development and commercialization of the PSCs. These challenges include hysteresis, reproducibility of efficient devices, toxicity as well as thermal and chemical stability. These factors directly or indirectly affect the stability of the PSCs. The stability of cells is a main hurdle in the commercialization of PSCs. Various approaches have been adopted with an aim to enhance the stability of PSCs, but they have failed to improve long-term performance of PSCs and the issue is still under debate. Of course, cost must also be kept in mind while considering the stability issues. If we take a close look at the energy levels/work function (given in Table 1) of the possible HTMs used in PSCs, it can be observed that spiro-OMeTad has least stability however it results in greater efficiency. P3HT with an $E_{\rm g}$ of 2 eV showed an efficiency of 20% and remained stable for 800 h. Similarly, the work function of the engineered PEDOT:PSS demonstrated better stability than the pristine PEDOT:PSS. Hence by gathering the facts regarding relation between performance and energy/level/work function, it can be inferred that LUMO/work function beyond 5 eV leads to better performance of the device.

Thermal and chemical stabilities are also very important issues which also need to be addressed properly, thermal treatment is required in the process of formation of perovskite crystals. Both annealing and storage temperatures are main diamine) (VNBP).

Review

factors due to which degradation in PSCs occurs. Thermal instability due to HTM can be reduced using HTM free perovskites solar cells. Excellent thermal stability has been reported with HTM free PSCs. For example, L. Etgar $et~al.^{154}$ were the first to report HTM-free MPSC with a 5.5% PCE. Later in 2014, they reported enhanced efficiency of HTM-free MPSC to 10.85%. Han and co-workers reported fully printable HTM-free MPSC based on triple mesoscopic layers of low-cost carbon counter electrode, mesoporous $\rm ZrO_2$ and $\rm TiO_2.^{156}$ The device exhibited good stability and a PCE of 6.64%. Li $et~al.^{31}$ performed some stability tests to check performance of the printable HTM-free MPSC using $(5-\rm AVA)_x(\rm MA)_{1-x}\rm PbI_3$. The devices remained stable when exposed outdoors in Jeddah, Saudia Arabia for a period of consecutive seven days. Furthermore, stable PSC was also re-

ported when the encapsulated device was thermally tested at

80-85 °C for 90 days. Moisture penetration in hole transporting

layer can be restricted by crosslinking the layer. Xu et al. 157 re-

ported thermally cross-linked arylamine derivative (N4,N4'-

di(naphthalen-1-yl)-N4,N4'-bis(4-vinylphenyl)biphenyl-4,4'-

Electron blocking layer (ETL) can also be used before the HTM layer and an HTM layer is used before ETL to restrict the overflow of electron and hole at either side as well as to reduce the moisture penetration. Xu *et al.*¹⁵⁷ used double layers of VNBP-MoO₃ and achieved better stability under harsh conditions. The hysteresis is also an important issue which might be closely related with long-term stability of the devices. There are few possible reasons for the hysteresis in organic perovskite solar cells which include charge trapping, There are lectricity highlighted in the capacitive effects. The properly controlling all these factors, hysteresis effects can be reduced.

The cost is another crucial factor that needs to be addressed beside the stability to introduce PSC technology to the commercial market for instance, the cost of purified spiro-OMeTAD is \sim \$500-1000 g⁻¹.81,166 The factors which affect the cost of HTMs include complex and costly systems required for purification process. Search for cost effective HTMs started since the first PSC was introduced. Zhang et al.167 reported a cost-effective dopant free P3HT as a replacement to spiro-MeOTAD. Later, Xiao and co-workers demonstrated a new class of solar cell with polyaniline (PANI) as a sensitizer and as a p-type hole transporting material.¹⁶⁸ In their work, they achieved a PCE of 7.34% along with long-term stability. Similarly, few researchers have employed inorganic hole transport materials. Christians et al.142 reported CuI as a hole transport material. Using cost effective, stable and solution-processable inorganic material, they showed a remarkable efficiency of 6.0% close to that of 7.9% (obtained for spiro-OMeTAD based device). However, there must be balance between the cost and efficiency.

To achieve best performance of PSCs, HTMs must fulfill following general requirements.

(1) The highest occupied molecular orbital (HOMO) energy level should be compatible with the valence band energy (VBE) of the perovskite.

- (2) For efficient hole transportation from perovskite absorber, HTMs must have sufficient charge carrier mobility (which ideally should be greater than 10^{-3} cm² V⁻¹ s⁻¹)
- (3) HTMs must have air, moisture, photochemical and thermal stability.
- (4) Ideally, HTMs should be solvable in various organic solvents and have exceptional film formation capability for device fabrication and processing.
- (5) HTMs should be low cost and have environmental friendly behavior.

In summary, up to now, a selection of organic, inorganic and hybrid HTMs have been reported in both standard and inverted PSC configurations. To enhance the PCE and stability of the PSCs, the following facts related to HTM must be considered. For the better PCEs, a good energy level alignment and interface compatibility should be taken into account, primarily. From the HTM-film quality optimization perspective, it is of utmost priority that a high-quality consistent HTM film must be prepared with less defects and desirable conductivity. Such HTMs can be achieved by optimizing or developing suitable deposition techniques. As far as the stability is concerned, additional emphasis should be put on interface engineering, compatibility and charge transfer kinetics. Furthermore, detailed understanding of interface charge transfers and recombination is necessary for developing new HTMs for stable and efficient PSCs.

8. Conclusion

During the past few years, intensive research interest from photovoltaic research community has been paid to PSCs. Perovskites are particularly considered for photovoltaic applications because they can be obtained from cheap earthabundant materials, processed in solution and show high device performance which is comparable with already implemented commercial technologies. Various techniques have been adopted to boost the power conversion efficiency (PCE) of PSCs. However, one key issue to approaching the market with any strategy is the long-term operational stability of PSC devices. In this review, the stability issues in PSCs and the role of HTMs on the stability and their proposed solutions have been discussed. It can be summarized that the integration of several types of approaches including interface engineering, composition engineering and development of hybrid HTMs and perovskite-inorganic HTM composites besides organic HTMs, might be important strategies for achieving high efficiency and better stability of PSCs.

Conflicts of interest

There are no conflicts to declare.

Acknowledgements

This work is supported by Qatar University Internal Grant No. QUCG-CAM-2018/19-1. The findings achieved herein are solely the responsibility of the authors.

References

- 1 M. A. Green, A. Ho-Baillie and H. J. Snaith, Nat. Photonics, 2014, 8, DOI: 10.1038/nphoton. 2014.2134.
- 2 A. Kojima, K. Teshima, T. Miyasaka and Y. Shirai, 214th ECS Meeting, ECS, 2014.
- 3 A. Kojima, K. Teshima, T. Miyasaka and Y. Shirai, 210th ECS Meeting, ECS, 2006.
- 4 A. Kojima, K. Teshima, Y. Shirai and T. Miyasaka, J. Am. Chem. Soc., 2009, 131, 6050-6051.
- 5 J.-H. Im, C.-R. Lee, J.-W. Lee, S.-W. Park and N.-G. Park, Nanoscale, 2011, 3, 4088-4093.
- 6 A. Yusoff, R. bin Mohd, J. Kim, J. Jang and M. K. Nazeeruddin, ChemSusChem, 2016, 9, 1736-1742.
- 7 H.-S. Kim, C.-R. Lee, J.-H. Im, K.-B. Lee, T. Moehl, A. Marchioro, S.-J. Moon, R. Humphry-Baker, J.-H. Yum and J. E. Moser, Sci. Rep., 2012, 2, 591.
- 8 M. M. Lee, J. Teuscher, T. Miyasaka, T. N. Murakami and H. J. Snaith, Science, 2012, 04, 1228604.
- 9 J. H. Heo, S. H. Im, J. H. Noh, T. N. Mandal, C.-S. Lim, J. A. Chang, Y. H. Lee, H.-j. Kim, A. Sarkar and M. K. Nazeeruddin, Nat. Photonics, 2013, 7, 486.
- 10 J. H. Noh, S. H. Im, J. H. Heo, T. N. Mandal and S. I. Seok, Nano Lett., 2013, 13, 1764-1769.
- 11 A. J. Huckaba, S. Gharibzadeh, M. Ralaiarisoa, C. Roldán-Carmona, N. Mohammadian, G. Grancini, Y. Lee, P. Amsalem, E. J. Plichta and N. Koch, Small Methods, 2017, 1, 1700250.
- 12 J. Burschka, N. Pellet, S.-J. Moon, R. Humphry-Baker, P. Gao, M. K. Nazeeruddin and M. Grätzel, Nature, 2013, 499, 316.
- 13 W. Tress, N. Marinova, T. Moehl, S. M. Zakeeruddin, M. K. Nazeeruddin and M. Grätzel, Energy Environ. Sci., 2015, 8, 995-1004.
- 14 A. Yusoff, R. bin Mohd, J. Kim, J. Jang and M. K. Nazeeruddin, ChemSusChem, 2016, 9, 1736-1742.
- 15 N. J. Jeon, J. H. Noh, Y. C. Kim, W. S. Yang, S. Ryu and S. I. Seok, Nat. Mater., 2014, 13, 897.
- 16 C. K. Teak, T. Olga, R. C. Cristina, I. Mine, G. Paul, G. Giulia, G. Peng, M. Tomasz, P. Wojciech, R. P. Y., T. Tomás and N. M. Khaja, Adv. Energy Mater., 2017, 7, 1601733.
- 17 N. J. Jeon, J. H. Noh, W. S. Yang, Y. C. Kim, S. Ryu, J. Seo and S. I. Seok, Nature, 2015, 517, 476.
- 18 P. Sanghyun, Q. Peng, L. Yonghui, C. K. Taek, G. Peng, G. Giulia, O. Emad, G. Paul, R. Kasparas, S. A. Al-Muhtaseb, L. Christian, K. Jaejung and N. M. Khaja, Adv. Mater., 2017, 29, 1606555.
- 19 A. D. Jodlowski, C. Roldán-Carmona, G. Grancini, M. Salado, M. Ralaiarisoa, S. Ahmad, N. Koch, L. Camacho, G. De Miguel and M. K. Nazeeruddin, Nat. Energy, 2017, 2, 972.
- 20 Y. Zhang, G. Grancini, Y. Feng, A. M. Asiri and M. K. Nazeeruddin, ACS Energy Lett., 2017, 2, 802-806.
- 21 M. Saliba, T. Matsui, J.-Y. Seo, K. Domanski, J.-P. Correa-Baena, M. K. Nazeeruddin, S. M. Zakeeruddin, W. Tress,

- A. Abate and A. Hagfeldt, Energy Environ. Sci., 2016, 9, 1989-1997.
- 22 D. B. Michele, D. E. Giorgio, G. Marina, D. I. Valerio, N. Stefanie, K. A. R. Srimath, G. Giulia, B. Maddalena, P. Mirko, B. J. M., C. Mario and P. Annamaria, Adv. Energy Mater., 2016, 6, 1501453.
- 23 M. Qian, M. Li, X.-B. Shi, H. Ma, Z.-K. Wang and L.-S. Liao, J. Mater. Chem. A, 2015, 3, 13533-13539.
- 24 M. Qian, M. Li, X.-B. Shi, H. Ma, Z.-K. Wang and L.-S. Liao, J. Mater. Chem. A, 2015, 3, 13533-13539.
- 25 Z.-K. Wang, M. Li, D.-X. Yuan, X.-B. Shi, H. Ma and L.-S. Liao, ACS Appl. Mater. Interfaces, 2015, 7, 9645-9651.
- 26 Y.-H. Lou and Z.-K. Wang, Nanoscale, 2017, 9, 13506–13514.
- 27 W. Jin-Miao, W. Zhao-Kui, L. Meng, Z. Cong-Cong, J. Lu-Lu, H. Ke-Hao, Y. Qing-Qing and L. Liang-Sheng, Adv. Energy Mater., 2018, 8, 1701688.
- 28 L. Meng, W. Zhao-Kui, Y. Ying-Guo, H. Yun, F. Shang-Lei, W. Jin-Miao, G. Xing-Yu and L. Liang-Sheng, Adv. Energy Mater., 2016, 6, 1601156.
- 29 Z.-K. Wang, X. Gong, M. Li, Y. Hu, J.-M. Wang, H. Ma and L.-S. Liao, ACS Nano, 2016, 10, 5479-5489.
- 30 G. Niu, X. Guo and L. Wang, J. Mater. Chem. A, 2015, 3, 8970-8980.
- 31 R. Yaoguang, L. Linfeng, M. Anyi, L. Xiong and H. Hongwei, Adv. Energy Mater., 2015, 5, 1501066.
- 32 R. Yaoguang, L. Linfeng, M. Anyi, L. Xiong and H. Hongwei, Adv. Energy Mater., 2015, 5, 1501066.
- 33 L. Zheng, Y.-H. Chung, Y. Ma, L. Zhang, L. Xiao, Z. Chen, S. Wang, B. Qu and Q. Gong, Chem. Commun., 2014, 50, 11196-11199.
- 34 N. Aristidou, I. Sanchez-Molina, T. Chotchuangchutchaval, M. Brown, L. Martinez, T. Rath and S. A. Haque, Angew. Chem., Int. Ed., 2015, 54, 8208-8212.
- 35 T. Leijtens, G. E. Eperon, S. Pathak, A. Abate, M. M. Lee and H. J. Snaith, Nat. Commun., 2013, 4, 2885.
- 36 S. Ito, S. Tanaka, K. Manabe and H. Nishino, J. Phys. Chem. C, 2014, 118, 16995-17000.
- 37 N. Chander, A. Khan, P. Chandrasekhar, E. Thouti, S. K. Swami, V. Dutta and V. K. Komarala, Appl. Phys. Lett., 2014, 105, 033904.
- 38 A. Dualeh, P. Gao, S. I. Seok, M. K. Nazeeruddin and M. Grätzel, Chem. Mater., 2014, 26, 6160-6164.
- 39 A. Pisoni, J. Jacimovic, O. S. Barisic, M. Spina, R. Gaál, L. Forró and E. Horváth, J. Phys. Chem. Lett., 2014, 5, 2488-2492.
- 40 S. N. Habisreutinger, T. Leijtens, G. E. Eperon, S. D. Stranks, R. J. Nicholas and H. J. Snaith, Nano Lett., 2014, 14, 5561-5568.
- 41 C. Bert, D. Jeroen, G. Nicolas, B. Aslihan, D. H. Jan, D. O. Lien, E. Anitha, V. Jo, M. Jean, M. Edoardo, A. F. De and B. Hans-Gerd, Adv. Energy Mater., 2015, 5, 1500477.
- 42 R. K. Misra, S. Aharon, B. Li, D. Mogilyansky, I. Visoly-Fisher, L. Etgar and E. A. Katz, J. Phys. Chem. Lett., 2015, 6, 326-330.
- 43 H. S. Kim, J. Y. Seo and N. G. Park, ChemSusChem, 2016, 9, 2528-2540.

Review

44 B. Philippe, B.-W. Park, R. Lindblad, J. Oscarsson,

S. Ahmadi, E. M. Johansson and H. k. Rensmo, *Chem. Mater.*, 2015, 27, 1720–1731.

- 45 B. Li, Y. Li, C. Zheng, D. Gao and W. Huang, *RSC Adv.*, 2016, 6, 38079–38091.
- 46 J. W. Lee, D. J. Seol, A. N. Cho and N. G. Park, *Adv. Mater.*, 2014, **26**, 4991–4998.
- 47 W. Feng, Y. Hui, X. Haihua and Z. Ni, *Adv. Funct. Mater.*, 2015, 25, 1120–1126.
- 48 Y. Fu, H. Zhu, A. W. Schrader, D. Liang, Q. Ding, P. Joshi, L. Hwang, X. Zhu and S. Jin, *Nano Lett.*, 2016, **16**, 1000– 1008.
- 49 Z. Wang, Z. Shi, T. Li, Y. Chen and W. Huang, *Angew. Chem., Int. Ed.*, 2017, **56**, 1190–1212.
- 50 J. Liu, Y. Wu, C. Qin, X. Yang, T. Yasuda, A. Islam, K. Zhang, W. Peng, W. Chen and L. Han, *Energy Environ. Sci.*, 2014, 7, 2963–2967.
- 51 J. Shi, J. Dong, S. Lv, Y. Xu, L. Zhu, J. Xiao, X. Xu, H. Wu, D. Li and Y. Luo, *Appl. Phys. Lett.*, 2014, **104**, 063901.
- 52 J. Yang, B. D. Siempelkamp, E. Mosconi, F. De Angelis and T. L. Kelly, *Chem. Mater.*, 2015, 27, 4229–4236.
- 53 Y. Chen, B. Li, W. Huang, D. Gao and Z. Liang, *Chem. Commun.*, 2015, **51**, 11997–11999.
- 54 S. N. Habisreutinger, D. P. McMeekin, H. J. Snaith and R. J. Nicholas, *APL Mater.*, 2016, 4, 091503.
- 55 L. Jin-Wook, K. Deok-Hwan, K. Hui-Seon, S. Seung-Woo, C. S. Min and P. Nam-Gyu, Adv. Energy Mater., 2015, 5, 1501310.
- 56 J. H. Noh, S. H. Im, J. H. Heo, T. N. Mandal and S. I. Seok, *Nano Lett.*, 2013, **13**, 1764–1769.
- 57 Improving the Long-Term Stability of Perovskite Solar Cells with a Porous Al₂O₃ Buffer Layer.
- 58 W. Li, W. Zhang, S. Van Reenen, R. J. Sutton, J. Fan, A. A. Haghighirad, M. B. Johnston, L. Wang and H. J. Snaith, *Energy Environ. Sci.*, 2016, **9**, 490–498.
- 59 R. Bart, K. C. Gödel, P. Sandeep, S. Aditya, B. J. P. Correa, B. D. Wilts, H. J. Snaith, W. Ulrich, G. Michael, S. Ullrich and A. Antonio, *Adv. Energy Mater.*, 2016, 6, 1501868.
- 60 I. Hwang and K. Yong, *ACS Appl. Mater. Interfaces*, 2016, **8**, 4226–4232.
- 61 C. Jiangzhao, S. Ja-Young and P. Nam-Gyu, *Adv. Energy Mater.*, 2018, **8**, 1702714.
- 62 P. Sanghyun, Q. Peng, L. Yonghui, C. K. Taek, G. Peng, G. Giulia, O. Emad, G. Paul, R. Kasparas, S. A. Al-Muhtaseb, L. Christian, K. Jaejung and N. M. Khaja, *Adv. Mater.*, 2017, 29, 1606555.
- 63 F. Zhang, Z. Wang, H. Zhu, N. Pellet, J. Luo, C. Yi, X. Liu, H. Liu, S. Wang and X. Li, *Nano Energy*, 2017, 41, 469–475.
- 64 H. Zheng, G. Liu, C. Zhang, L. Zhu, A. Alsaedi, T. Hayat, X. Pan and S. Dai, *Sol. Energy*, 2018, **159**, 914–919.
- 65 R. Azmi, S. Y. Nam, S. Sinaga, Z. A. Akbar, C.-L. Lee, S. C. Yoon, I. H. Jung and S.-Y. Jang, *Nano Energy*, 2018, 44, 191–198.
- 66 Q. Chen, et al., Dyes Pigm., 2017, 147(suppl. C), 113-119.
- 67 M.-D. Zhang, B.-H. Zheng, Q.-F. Zhuang, C.-Y. Huang, H. Cao, M.-D. Chen and B. Wang, *Dyes Pigm.*, 2017, **146**, 589–595.

- 68 E. Nouri, et al., Electrochim. Acta, 2016, 222(suppl. C), 875–880.
- 69 X. Zong, W. Qiao, Y. Chen, Z. Sun, M. Liang and S. Xue, *Tetrahedron*, 2017, 73, 3398–3405.
- 70 J.-J. Guo, et al., Sol. Energy, 2017, 155(suppl. C), 121-129.
- 71 Y. Wei, et al., Appl. Surf. Sci., 2018, 427(part B), 782-790.
- 72 S. K. Muduli, et al., J. Power Sources, 2017, 371(suppl. C), 156–161.
- 73 J. Niu, et al., Org. Electron., 2017, 48(suppl. C), 165-171.
- 74 K. Im, et al., Chem. Eng. J., 2017, 330(suppl. C), 698-705.
- 75 L. Calió, et al., Sol. Energy Mater. Sol. Cells, 2017, 163(suppl. C), 237–241.
- 76 L. Yang, Y. Yan, F. Cai, J. Li and T. Wang, Sol. Energy Mater. Sol. Cells, 2017, 163, 210–217.
- 77 M. Sun, et al., Appl. Surf. Sci., 2017, 416(suppl. C), 124-132.
- 78 P. Qi, et al., Synth. Met., 2017, 226(suppl. C), 1-6.
- 79 G. Gong, N. Zhao, J. Li, F. Li, J. Chen, Y. Shen, M. Wang and G. Tu, Org. Electron., 2016, 35, 171–175.
- 80 R. Sandoval-Torrientes, I. Zimmermann, J. Calbo, J. Aragó, J. Santos, E. Ortí, N. Martín and M. Nazeeruddin, *J. Mater. Chem. A*, 2018, 6, 5944–5951.
- 81 P. Vivo, J. K. Salunke and A. Priimagi, *Materials*, 2017, 10, 1087.
- 82 N. J. Jeon, J. Lee, J. H. Noh, M. K. Nazeeruddin, M. Grätzel and S. I. Seok, *J. Am. Chem. Soc.*, 2013, **135**, 19087–19090.
- 83 C. Huang, W. Fu, C.-Z. Li, Z. Zhang, W. Qiu, M. Shi, P. Heremans, A. K.-Y. Jen and H. Chen, *J. Am. Chem. Soc.*, 2016, **138**, 2528–2531.
- 84 R. Grisorio, R. Iacobellis, A. Listorti, L. De Marco, M. P. Cipolla, M. Manca, A. Rizzo, A. Abate, G. Gigli and G. P. Suranna, ACS Appl. Mater. Interfaces, 2017, 9, 24778– 24787.
- 85 K. Rakstys, A. Abate, M. I. Dar, P. Gao, V. Jankauskas, G. n. Jacopin, E. Kamarauskas, S. Kazim, S. Ahmad and M. Grätzel, *J. Am. Chem. Soc.*, 2015, 137, 16172–16178.
- 86 D. Shinde, J. K. Salunke, N. R. Candeias, F. Tinti, M. Gazzano, P. Wadgaonkar, A. Priimagi, N. Camaioni and P. Vivo, Sci. Rep., 2017, 7, 46268.
- 87 R. Grisorio, B. Roose, S. Colella, A. Listorti, G. P. Suranna and A. Abate, *ACS Energy Lett.*, 2017, 2, 1029–1034.
- 88 L. Xuepeng, K. Fantai, G. Rahim, J. Shengli, C. Wangchao, Y. Ting, H. Tasawar, A. Ahmed, G. Fuling, T. Zhan'ao, C. Jian and D. Songyuan, *Energy Technol.*, 2017, 5, 1788– 1794.
- 89 K. Rakstys, S. Paek, M. Sohail, P. Gao, K. T. Cho, P. Gratia, Y. Lee, K. H. Dahmen and M. K. Nazeeruddin, *J. Mater. Chem. A*, 2016, 4, 18259–18264.
- 90 Z. Iwan, U. M. Javier, G. Paul, A. Juan, G. Giulia, M. O. Agustín, O. Enrique, M. Nazario and N. M. Khaja, Adv. Energy Mater., 2017, 7, 1601674.
- 91 K. Do, H. Choi, K. Lim, H. Jo, J. W. Cho, M. K. Nazeeruddin and J. Ko, *Chem. Commun.*, 2014, **50**, 10971–10974.
- 92 K. Lim, M.-S. Kang, Y. Myung, J.-H. Seo, P. Banerjee, T. J. Marks and J. Ko, *J. Mater. Chem. A*, 2016, 4, 1186–1190.
- 93 M. O. Agustín, Z. Iwan, G. B. Inés, G. Paul, R. C. Cristina, A. Sadig, G. Michael, N. M. Khaja and M. Nazario, *Angew. Chem., Int. Ed.*, 2016, 55, 6270–6274.

RSC Advances

94 I. García-Benito, I. Zimmermann, J. Urieta-Mora, J. Aragó, A. Molina-Ontoria, E. Ortí, N. Martín and M. K. Nazeeruddin, J. Mater. Chem. A, 2017, 5, 8317–8324.

- 95 S. Paek, M. A. Rub, H. Choi, S. A. Kosa, K. A. Alamry, J. W. Cho, P. Gao, J. Ko, A. M. Asiri and M. K. Nazeeruddin, *Nanoscale*, 2016, 8, 6335–6340.
- 96 R. Kasparas, S. Michael, G. Peng, G. Paul, K. Egidijus, P. Sanghyun, J. Vygintas and N. M. Khaja, *Angew. Chem.*, *Int. Ed.*, 2016, 55, 7464–7468.
- 97 W. Ya-Kun, Y. Zhong-Cheng, S. Guo-Zheng, L. Yong-Xi, L. Qian, H. Fei, S. Bao-Quan, J. Zuo-Quan and L. Liang-Sheng, *Adv. Funct. Mater.*, 2016, **26**, 1375–1381.
- 98 R. S. Sudhaker, G. Kumarasamy, H. J. Hyuck, I. S. Hyuk, K. C. Su, K. Dong-Ho, M. J. Hun, L. J. Yong, S. Myungkwan and J. Sung-Ho, *Adv. Mater.*, 2016, **28**, 686–693.
- 99 R. Tiazkis, S. Paek, M. Daskeviciene, T. Malinauskas, M. Saliba, J. Nekrasovas, V. Jankauskas, S. Ahmad, V. Getautis and M. K. Nazeeruddin, Sci. Rep., 2017, 7, 150.
- 100 D. Bi, B. Xu, P. Gao, L. Sun, M. Grätzel and A. Hagfeldt, *Nano Energy*, 2016, 23, 138–144.
- 101 B. Xu, J. Zhang, Y. Hua, P. Liu, L. Wang, C. Ruan, Y. Li, G. Boschloo, E. M. Johansson and L. Kloo, *Chem*, 2017, 2, 676–687.
- 102 T. Malinauskas, M. Saliba, T. Matsui, M. Daskeviciene, S. Urnikaite, P. Gratia, R. Send, H. Wonneberger, I. Bruder and M. Graetzel, *Energy Environ. Sci.*, 2016, 9, 1681–1686.
- 103 M. Saliba, S. Orlandi, T. Matsui, S. Aghazada, M. Cavazzini, J.-P. Correa-Baena, P. Gao, R. Scopelliti, E. Mosconi and K.-H. Dahmen, *Nat. Energy*, 2016, 1, 15017.
- 104 W. S. Yang, J. H. Noh, N. J. Jeon, Y. C. Kim, S. Ryu, J. Seo and S. I. Seok, *Science*, 2015, 348, 1234–1237.
- 105 P. Gratia, A. Magomedov, T. Malinauskas, M. Daskeviciene, A. Abate, S. Ahmad, M. Grätzel, V. Getautis and M. K. Nazeeruddin, *Angew. Chem., Int. Ed.*, 2015, 54, 11409–11413.
- 106 T. Leijtens, T. Giovenzana, S. N. Habisreutinger, J. S. Tinkham, N. K. Noel, B. A. Kamino, G. Sadoughi, A. Sellinger and H. J. Snaith, ACS Appl. Mater. Interfaces, 2016, 8, 5981–5989.
- 107 S. D. Sung, M. S. Kang, I. T. Choi, H. M. Kim, H. Kim, M. Hong, H. K. Kim and W. I. Lee, *Chem. Commun.*, 2014, 50, 14161–14163.
- 108 J. Wang, Y. Chen, F. Li, X. Zong, J. Guo, Z. Sun and S. Xue, *Electrochim. Acta*, 2016, **210**, 673–680.
- 109 M. S. Kang, S. D. Sung, I. T. Choi, H. Kim, M. Hong, J. Kim, W. I. Lee and H. K. Kim, *ACS Appl. Mater. Interfaces*, 2015, 7, 22213–22217.
- 110 M. Daskeviciene, S. Paek, Z. Wang, T. Malinauskas, G. Jokubauskaite, K. Rakstys, K. T. Cho, A. Magomedov, V. Jankauskas and S. Ahmad, *Nano Energy*, 2017, 32, 551– 557
- 111 C. Zhiliang, L. Hui, Z. Xiaolu, Z. Qi, L. Zhanfeng, H. Yuying and F. Guojia, *ChemSusChem*, 2017, **10**, 3111–3117.

- 112 Z. Hongwei, Z. Fei, L. Xicheng, S. Mengna, H. Jianlei, Y. Jing, W. Shirong, X. Yin and L. Xianggao, *Energy Technol.*, 2017, 5, 1257–1264.
- 113 Z. Linna, S. Yahan, W. Rui, L. Debei, Z. Cheng, S. Qunliang and W. Fei, *Chem.–Eur. J.*, 2017, **23**, 4373–4379.
- 114 X. Bo, S. Esmaeil, L. Peng, Z. Jinbao, T. Haining, V. Nick, B. Gerrit, K. Lars, H. Anders and S. Licheng, *Adv. Mater.*, 2014, 26, 6629–6634.
- 115 H. Wang, A. D. Sheikh, Q. Feng, F. Li, Y. Chen, W. Yu, E. Alarousu, C. Ma, M. A. Haque and D. Shi, ACS *Photonics*, 2015, 2, 849–855.
- 116 F. Di Giacomo, S. Razza, F. Matteocci, A. D'Epifanio, S. Licoccia, T. M. Brown and A. Di Carlo, *J. Power Sources*, 2014, **251**, 152–156.
- 117 E. Gabrielsson, H. Ellis, S. Feldt, H. Tian, G. Boschloo, A. Hagfeldt and L. Sun, *Adv. Energy Mater.*, 2013, **3**, 1647–1656.
- 118 F. Wu, Y. Ji, R. Wang, Y. Shan and L. Zhu, *Dyes Pigm.*, 2017, 143, 356–360.
- 119 X. Li, M. Cai, Z. Zhou, K. Yun, F. Xie, Z. Lan, J. Hua and L. Han, *J. Mater. Chem. A*, 2017, **5**, 10480–10485.
- 120 M. Petrus, T. Bein, T. Dingemans and P. Docampo, *J. Mater. Chem. A*, 2015, 3, 12159–12162.
- 121 W. S. Yang, B.-W. Park, E. H. Jung, N. J. Jeon, Y. C. Kim, D. U. Lee, S. S. Shin, J. Seo, E. K. Kim and J. H. Noh, *Science*, 2017, 356, 1376–1379.
- 122 X. Zheng, B. Chen, J. Dai, Y. Fang, Y. Bai, Y. Lin, H. Wei, X. C. Zeng and J. Huang, *Nat. Energy*, 2017, 2, 17102.
- 123 Z. Zhuang, Y. Li, D. Qi, C. Zhao and H. Na, *Sens. Actuators*, *B*, 2017, **242**, 801–809.
- 124 W. Ma, C. Yang, X. Gong, K. Lee and A. J. Heeger, *Adv. Funct. Mater.*, 2005, **15**, 1617–1622.
- 125 H. Yoon, S. M. Kang, J.-K. Lee and M. Choi, *Energy Environ. Sci.*, 2016, **9**, 2262–2266.
- 126 L. Kyung-Geun, A. Soyeong, K. Hobeom, C. Mi-Ri, H. D. Ho and L. Tae-Woo, *Adv. Mater. Interfaces*, 2016, 3, 1500678.
- 127 K.-G. Lim, S. Ahn, Y.-H. Kim, Y. Qi and T.-W. Lee, *Energy Environ. Sci.*, 2016, **9**, 932–939.
- 128 K. G. Lim, H. B. Kim, J. Jeong, H. Kim, J. Y. Kim and T. W. Lee, *Adv. Mater.*, 2014, **26**, 6461–6466.
- 129 A. Dubey, N. Adhikari, S. Venkatesan, S. Gu, D. Khatiwada, Q. Wang, L. Mohammad, M. Kumar and Q. Qiao, *Sol. Energy Mater. Sol. Cells*, 2016, 145, 193–199.
- 130 M. Wong-Stringer, J. E. Bishop, J. A. Smith, D. K. Mohamad, A. J. Parnell, V. Kumar, C. Rodenburg and D. G. Lidzey, *J. Mater. Chem. A*, 2017, 5, 15714–15723.
- 131 Z. Yu, Y. Zhang, X. Jiang, X. Li, J. Lai, M. Hu, M. Elawad, G. G. Gurzadyan, X. Yang and L. Sun, RSC Adv., 2017, 7, 27189–27197.
- 132 Z. Zhou, Y. Zhao, C. Zhang, D. Zou, Y. Chen, Z. Lin, H. Zhen and Q. Ling, *J. Mater. Chem. A*, 2017, 5, 6613–6621.
- 133 J. Liu, Q. Ge, W. Zhang, J. Ma, J. Ding, G. Yu and J. Hu, *Nano Res.*, 2018, **11**, 185–194.
- 134 E. A. Gaml, A. Dubey, K. M. Reza, M. N. Hasan, N. Adhikari, H. Elbohy, B. Bahrami, H. Zeyada, S. Yang and Q. Qiao, *Sol. Energy Mater. Sol. Cells*, 2017, **168**, 8–13.

Review

- 135 K. Rakstys, S. Paek, P. Gao, P. Gratia, T. Marszalek, G. Grancini, K. T. Cho, K. Genevicius, V. Jankauskas and W. Pisula, *J. Mater. Chem. A*, 2017, 5, 7811–7815.
- 136 J. H. Heo, S. Park, S. H. Im and H. J. Son, *ACS Appl. Mater. Interfaces*, 2017, **9**, 39511–39518.
- 137 J. Lee, M. Malekshahi Byranvand, G. Kang, S. Y. Son, S. Song, G.-W. Kim and T. Park, *J. Am. Chem. Soc.*, 2017, 139, 12175–12181.
- 138 A. S. Subbiah, A. Halder, S. Ghosh, N. Mahuli, G. Hodes and S. K. Sarkar, *J. Phys. Chem. Lett.*, 2014, 5, 1748–1753.
- 139 K.-C. Wang, P.-S. Shen, M.-H. Li, S. Chen, M.-W. Lin, P. Chen and T.-F. Guo, ACS Appl. Mater. Interfaces, 2014, 6, 11851–11858.
- 140 Z. Liu, A. Zhu, F. Cai, L. Tao, Y. Zhou, Z. Zhao, Q. Chen, Y.-B. Cheng and H. Zhou, *J. Mater. Chem. A*, 2017, 5, 6597–6605.
- 141 P. H. Duc, W. Zhifang, L. K. Ono, M. Sergei, F. Krishna, M. Nunzio, Q. Yabing and S. Prashant, Adv. Electron. Mater., 2017, 3, 1700139.
- 142 J. A. Christians, R. C. Fung and P. V. Kamat, *J. Am. Chem. Soc.*, 2013, **136**, 758–764.
- 143 B. A. Nejand, V. Ahmadi, S. Gharibzadeh and H. R. Shahverdi, *ChemSusChem*, 2016, 9, 302–313.
- 144 Y. Wang, Z. Xia, J. Liang, X. Wang, Y. Liu, C. Liu, S. Zhang and H. Zhou, *Semicond. Sci. Technol.*, 2015, **30**, 054004.
- 145 P. Qin, S. Tanaka, S. Ito, N. Tetreault, K. Manabe, H. Nishino, M. K. Nazeeruddin and M. Grätzel, *Nat. Commun.*, 2014, 5, 3834.
- 146 V. E. Madhavan, I. Zimmermann, C. Roldán-Carmona, G. Grancini, M. Buffiere, A. Belaidi and M. K. Nazeeruddin, ACS Energy Lett., 2016, 1, 1112–1117.
- 147 Y. S. Kwon, J. Lim, H.-J. Yun, Y.-H. Kim and T. Park, Energy Environ. Sci., 2014, 7, 1454–1460.
- 148 X. Liang, C. Wang, M. Wu, Y. Wu, F. Zhang, Z. Han, X. Lu, K. Guo and Y.-M. Zhao, *Tetrahedron*, 2017, 73, 7115–7121.
- 149 F. Xie, C.-C. Chen, Y. Wu, X. Li, M. Cai, X. Liu, X. Yang and L. Han, *Energy Environ. Sci.*, 2017, **10**, 1942–1949.
- 150 H. Li, K. Fu, A. Hagfeldt, M. Grätzel, S. G. Mhaisalkar and A. C. Grimsdale, *Angew. Chem., Int. Ed.*, 2014, 53, 4085–4088.

- 151 C. Laura, K. Samrana, G. Michael and A. Shahzada, Angew. Chem., Int. Ed., 2016, 55, 14522–14545.
- 152 Y. Ze and S. Licheng, Adv. Energy Mater., 2015, 5, 1500213.
- 153 Z. H. Bakr, Q. Wali, A. Fakharuddin, L. Schmidt-Mende, T. M. Brown and R. Jose, *Nano Energy*, 2017, **34**, 271–305.
- 154 L. Etgar, P. Gao, Z. Xue, Q. Peng, A. K. Chandiran, B. Liu, M. K. Nazeeruddin and M. Grätzel, *J. Am. Chem. Soc.*, 2012, 134, 17396–17399.
- 155 S. Aharon, S. Gamliel, B. El Cohen and L. Etgar, *Phys. Chem. Chem. Phys.*, 2014, **16**, 10512–10518.
- 156 Z. Ku, Y. Rong, M. Xu, T. Liu and H. Han, *Sci. Rep.*, 2013, 3, 3132.
- 157 J. Xu, O. Voznyy, R. Comin, X. Gong, G. Walters, M. Liu, P. Kanjanaboos, X. Lan and E. H. Sargent, Adv. Mater., 2016, 28, 2807–2815.
- 158 N. K. Elumalai, M. A. Mahmud, D. Wang and A. Uddin, Energies, 2016, 9, 861.
- 159 D. A. Egger, E. Edri, D. Cahen and G. Hodes, *J. Phys. Chem. Lett.*, 2015, **6**, 279–282.
- 160 W. Tress, N. Marinova, T. Moehl, S. M. Zakeeruddin, M. K. Nazeeruddin and M. Grätzel, *Energy Environ. Sci.*, 2015, 8, 995–1004.
- 161 J. Wei, Y. Zhao, H. Li, G. Li, J. Pan, D. Xu, Q. Zhao and D. Yu, J. Phys. Chem. Lett., 2014, 5, 3937–3945.
- 162 H.-W. Chen, N. Sakai, M. Ikegami and T. Miyasaka, *J. Phys. Chem. Lett.*, 2014, 6, 164–169.
- 163 J. M. Frost, K. T. Butler, F. Brivio, C. H. Hendon, M. Van Schilfgaarde and A. Walsh, *Nano Lett.*, 2014, 14, 2584–2590.
- 164 R. S. Sanchez, V. Gonzalez-Pedro, J.-W. Lee, N.-G. Park, Y. S. Kang, I. Mora-Sero and J. Bisquert, *J. Phys. Chem. Lett.*, 2014, 5, 2357–2363.
- 165 O. Almora, I. Zarazua, E. Mas-Marza, I. Mora-Sero, J. Bisquert and G. Garcia-Belmonte, J. Phys. Chem. Lett., 2015, 6, 1645–1652.
- 166 A. Krishna and A. C. Grimsdale, *J. Mater. Chem. A*, 2017, 5, 16446–16466.
- 167 Z. Meng, L. Miaoqiang, Y. Hua, Y. Jung-Ho, W. Qiong and W. Lianzhou, *Chem.-Eur. J.*, 2015, 21, 434–439.
- 168 Y. Xiao, G. Han, Y. Chang, H. Zhou, M. Li and Y. Li, *J. Power Sources*, 2014, **267**, 1–8.